SUPPLEMENTARY INFORMATION

Supplementary information includes nine figures, two tables, supplementary methods and references.

SUPPLEMENTARY FIGURES

Figure S1. RNA binding proteins that modulate *Bcl-x* alternative splicing. Diagram of *cis* and *trans*-acting elements localized in exon 2 that regulate *Bcl-x* splicing. Light grey boxes represent enhancers, while dark grey boxes represent silencers. The *pointed* and *flat arrows* indicate positive and negative regulation, respectively. SB1 is a 361 nt-long element located at the 5' of exon 2, possessing a repressive activity on the Bcl-xS splice site (Revil et al., 2007). CRCE1, bound by SAP155, and CRCE2 are two silencers located on both sides of the Bcl-xS splice site (Massiello et al., 2006; Massiello et al., 2004). RBM25 binds a B1AG enhancer of Bcl-xS (Zhou et al., 2008), whereas hnRNP K inhibits the production of Bcl-xS upon binding to the B1u element (Revil et al., 2009). hnRNP F and H stimulate Bcl-xS when bound to the B2G enhancer element (Garneau et al., 2005). SRp30c acts on two consecutive elements (AM2 and ML2) to encourage Bcl-xL expression (Cloutier et al., 2008). Although the *cis*-elements required for their activity are currently not known, SC35 and a hnRNP A1/Sam68 complex act as Bcl-xS positive regulators (Merdzhanova et al., 2008; Paronetto et al., 2007).

Figure S2. The knockdown of eIF4A3, Acinus and SAP18 shift *Bcl-x* splicing towards an increased production of Bcl-x_S. RT-PCR analysis of *Bcl-x* alternative splicing following the knockdown of EJC components. 293 and HeLa cells were transfected with siRNAs targeting

eIF4A3, Acinus, SAP18 and MLN51. Total RNA was extracted 72 hours later. RT-PCR analysis of ^{32}P-labeled products was carried out, a portion of which is shown here. The products were quantitated and the values were plotted in Figure 1C.

Figure S3. The knockdown of eIF4A3, Y14 and RNPS1 do not significantly alter the expression levels of known *Bcl-x* splicing regulators. Following transfection of 293 and HeLa cells, cell lysates were prepared 48 or 72 hours later, and analyzed by Western blots to monitor the levels of the known *Bcl-x* splicing regulators hnRNP K, hnRNP F/H, hnRNP A1 and SRp30c (left panels). β-actin was used as a loading control. The same cell samples were used for RNA extraction and RT-PCR analysis of *Bcl-x* alternative splicing (bar graphs on the right).

Figure S4. The shifts in *Bcl-x* splicing induced by knocking down Y14 and RNPS1 require active transcription. RT-PCR analysis of *Bcl-x* alternative splicing in 293 and HeLa cells transfected with siRNAs targeting Y14 and RNPS1. After 24 hours, cells were treated with actinomycin D or DRB. Twenty-four hours later, total RNA was extracted and RT-PCR was performed to amplify both *Bcl-x* splice forms.

Figure S5. RNPS1 modulates Bcl-x pre-mRNA splicing in a SB1-dependent manner, while core EJC factors and PYM activities are independent of SB1. Gels displaying a RT-PCR analysis conducted on transcripts derived from *Bcl-x* minigenes following the knockdown/overexpression of EJC components. 293 cells were treated with siRNAs targeting RNPS1, Y14, eIF4A3 or PYM and transfected with *Bcl-x* minigenes, or co-transfected with FLAG-RNPS1, FLAG-Y14 or FLAG-PYM constructs with the minigenes. The values extracted from these experiments are part of Figures 2B and 2C.

Figure S6. EJC components associate with the *Bcl-x* pre-mRNA and modulate its alternative splicing. (A) Gels displaying RT-PCR analyses of *Bcl-x* alternative splicing *in vitro*, following incubation of various *Bcl-x* mutant transcripts in a HeLa nuclear extract supplemented with increasing amount of His-tagged recombinant eIF4A3 or Magoh-Y14ΔN. These results were part of the graphs presented in Figure 3E. (B) Following the incubation of the various *Bcl-x* mutant pre-mRNAs in a HeLa nuclear extract, radiolabeled RNA was immunoprecipitated with anti-Y14. The percentage of immunoprecipitated labeled RNA (relative to input and subtracted from a mock immunoprecipitation performed with each pre-mRNA) is plotted. (C) Following the incubation of X2 (+SB1) and X2.13 (-SB1) *Bcl-x* mutant transcripts in a HeLa nuclear extract, radiolabeled RNA was immunoprecipitated with anti-RNPS1 (Abcam ab56806). The percentage of immunoprecipitated labeled RNA (relative to input and subtracted from a mock immunoprecipitation performed with each pre-mRNA) is plotted.

Figure S7. Isoform changes detected on the Bcl-x, Mcl1 and Bim proteins.

Protein samples from 293 and HeLa cells treated with various siRNAs were analyzed by western blotting for corresponding shifts in protein isoforms. Anti-GAPDH was used as a loading control. A slight increase in Bcl-xS is observed upon knockdown of Y14 and RNPS1. In the case of Mcl1, although the pro-apoptotic Mcl1-S variant could not be detected, we noted a reduction in the level of the larger anti-apoptotic product Mcl1-L when eIF4A3 was inhibited. Likewise, the longest and least pro-apoptotic BimEL isoform is reduced upon knockdown of RNPS1.

Figure S8. The knockdown of Y14, RNPS1 and eIF4A3 induce PARP cleavage and the shifts in *Bcl-x* splicing induced by the depletion of Y14 and RNPS1 are independent of caspases.

293 and HeLa cells were transfected with siRNAs targeting Y14 and RNPS1 for 24 hours or were pre-treated for 24 hours with vinorelbine, a known caspases activator. Cells were then treated or not with the general caspases inhibitor z-VAD-fmk. After 24 hours, total proteins and RNA were extracted. (A) Western blot analysis of PARP cleavage indicating that all treatment stimulated caspases-dependent PARP cleavage. (B) 293 and HeLa cells were transfected with a siRNA targeting eIF4A3 and PARP cleavage was assessed by Western blot analysis. (C) RT-PCR analysis of *Bcl-x* alternative splicing in 293 and HeLa cells indicating that caspases inhibition does not alter the *Bcl-x* splicing shift induced by siY14 and siRNPS1.

Figure S9. The knockdowns of Y14, eIF4A3 and RNPS1 significantly induce apoptosis in PC-3 cells. Annexin-V assay in PC-3 cells transfected with siRNAs targeting EJC components. Cells were immunostained for annexin-V (red) and nuclei were labelled with Hoechst (blue) (Sudo et al., 2010). The percentage of apoptotic cells was quantitated (bottom graph) and compared to various controls (lipofectamine alone, control siRNA and a variety of siRNAs (2 siRNAs each) targeting Y14, eIF4A3 and the RNA binding proteins CDC5L, EWSR1 and KHSRP that display splicing regulatory activity (Dutertre et al., 2010; Lleres et al., 2010; Min et al., 1997), but do not affect *Bcl-x* alternative splicing (Table S1).

SUPPLEMENTARY TABLES

Table S1. Impact of depleting various RNA binding proteins on the *Bcl-x* splicing ratio. Cells were transfected for 96 hours with siRNAs. The Bcl-xL and Bcl-xS mRNA isoforms were co-amplified by RT-PCR in the presence of ^{32}P-dCTP. Products were fractionated by electrophoresis and quantitated by autoradiography. A change in the percentage of the Bcl-xS product was considered

significant (and indicated with an X) only if it was superior to 10% and detected with both siRNAs. The knockdown efficiency was assessed by qRT-PCR and a gray background indicates a decrease in mRNA expression superior to 50%.

Table S2. Sequence of siRNAs used for the knockdown of RNA binding proteins. The list contains all siRNAs used in the original screen as well as siRNAs against several EJC components used thereafter.

SUPPLEMENTARY METHODS

Cell culture and transfections. HeLa and 293 cells were grown and transfected in standard conditions, as described in the "Material and Methods" section of the current paper.

Antibodies. Antibodies used for this complementary analysis were the following: α-Bcl-x (Genetex #105661), α-Bim (Cell Signaling #2819), α-Mcl1 (Santa Cruz Biotechnology #MCL1S-19), α-actin (Sigma #A2066), α-GAPDH (Novus Biologicals #NB300-221). Rabbit polyclonal serum was raised against a peptide unique to the hnRNP A1 protein (ASASSSQRGR, α-hnRNP A1). Peptide synthesis and antibody production was carried out initially by the Service de Séquence de Peptide de l'Est du Québec, (CHUL, Ste-Foy, Quebec, Canada). For α-hnRNP F, α-hnRNP H and α-SRp30c antibodies , rabbit polyclonal sera were raised against a peptide unique to the hnRNP F protein (MMLGPEGGEGFVVKC), hnRNP H protein (QVLQENSSDFQSNIAC) and SRp30c protein (MSGWADERGGEGDGR). Peptide synthesis and antibody production was carried out initially by Chemicon International (Temecula, CA, USA). α-hnRNP K was a gift from G. Dreyfuss.

Chemicals and inhibitors. Actinomycin D and DRB were purchased from Calbiochem.

PARP cleavage assay. The inhibitor of caspases z-VAD-fmk (Calbiochem) was used at a final concentration of 50 μM and cells were treated for 24 hours after vinorelbine or the siRNA treatments was initiated. Two-third of the cells from each well were then collected for protein extraction and the rest was used for RNA extraction. Whole cells extracts were prepared in Laemmli sample buffer. Protein samples (20 μg/well) were fractionated on a 9% SDS-PAGE (29:1 acrylamide:bisacrylamide) and transferred onto a Hybond-C nitrocellulose membrane. Immunodetection was performed according to standard protocols using a dilution of 1:500 of the rabbit anti-PARP antibody (Biosource) and 1:5000 of the HRP-conjugated anti-rabbit secondary antibody (Amersham Biosciences).

SUPPLEMENTARY REFERENCES

Cloutier, P., Toutant, J., Shkreta, L., Goekjian, S., Revil, T., and Chabot, B. (2008). Antagonistic effects of the SRp30c protein and cryptic 5' splice sites on the alternative splicing of the apoptotic regulator Bcl-x. J Biol Chem *283*, 21315-21324.

Dutertre, M., Sanchez, G., De Cian, M.C., Barbier, J., Dardenne, E., Gratadou, L., Dujardin, G., Le Jossic-Corcos, C., Corcos, L., and Auboeuf, D. (2010). Cotranscriptional exon skipping in the genotoxic stress response. Nat Struct Mol Biol *17*, 1358-1366.

Garneau, D., Revil, T., Fisette, J.F., and Chabot, B. (2005). Heterogeneous nuclear ribonucleoprotein F/H proteins modulate the alternative splicing of the apoptotic mediator Bcl-x. J Biol Chem *280*, 22641-22650.

Lleres, D., Denegri, M., Biggiogera, M., Ajuh, P., and Lamond, A.I. (2010). Direct interaction between hnRNP-M and CDC5L/PLRG1 proteins affects alternative splice site choice. EMBO Rep *11*, 445-451.

Massiello, A., Roesser, J.R., and Chalfant, C.E. (2006). SAP155 Binds to ceramide-responsive RNA cis-element 1 and regulates the alternative 5' splice site selection of Bcl-x pre-mRNA. Faseb J *20*, 1680-1682.

Massiello, A., Salas, A., Pinkerman, R.L., Roddy, P., Roesser, J.R., and Chalfant, C.E. (2004). Identification of two RNA cis-elements that function to regulate the 5' splice site selection of Bcl-x pre-mRNA in response to ceramide. J Biol Chem *279*, 15799-15804.

Merdzhanova, G., Edmond, V., De Seranno, S., Van den Broeck, A., Corcos, L., Brambilla, C., Brambilla, E., Gazzeri, S., and Eymin, B. (2008). E2F1 controls alternative splicing pattern of genes involved in apoptosis through upregulation of the splicing factor SC35. Cell Death Differ *15*, 1815-1823.

Min, H., Turck, C.W., Nikolic, J.M., and Black, D.L. (1997). A new regulatory protein, KSRP, mediates exon inclusion through an intronic splicing enhancer. Genes Dev *11*, 1023-1036.
Paronetto, M.P., Achsel, T., Massiello, A., Chalfant, C.E., and Sette, C. (2007). The RNA-binding protein Sam68 modulates the alternative splicing of Bcl-x. J Cell Biol *176*, 929-939.
Revil, T., Pelletier, J., Toutant, J., Cloutier, A., and Chabot, B. (2009). Heterogeneous nuclear ribonucleoprotein K represses the production of pro-apoptotic Bcl-xS splice isoform. J Biol Chem *284*, 21458-21467.
Revil, T., Toutant, J., Shkreta, L., Garneau, D., Cloutier, P., and Chabot, B. (2007). Protein kinase C-dependent control of Bcl-x alternative splicing. Mol Cell Biol *27*, 8431-8441.
Sudo, H., Tsuji, A.B., Sugyo, A., Kohda, M., Sogawa, C., Yoshida, C., Harada, Y.N., Hino, O., and Saga, T. (2010). Knockdown of COPA, identified by loss-of-function screen, induces apoptosis and suppresses tumor growth in mesothelioma mouse model. Genomics *95*, 210-216.
Zhou, A., Ou, A.C., Cho, A., Benz, E.J., Jr., and Huang, S.C. (2008). Novel splicing factor RBM25 modulates Bcl-x pre-mRNA 5' splice site selection. Mol Cell Biol *28*, 5924-5936.

Supplementary figures

S1

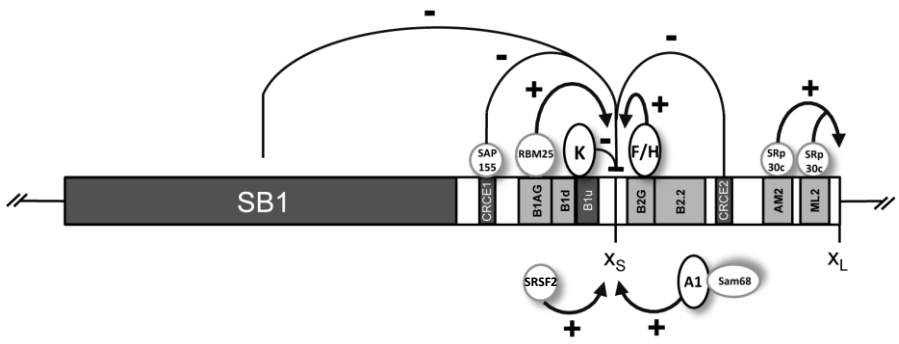

S2

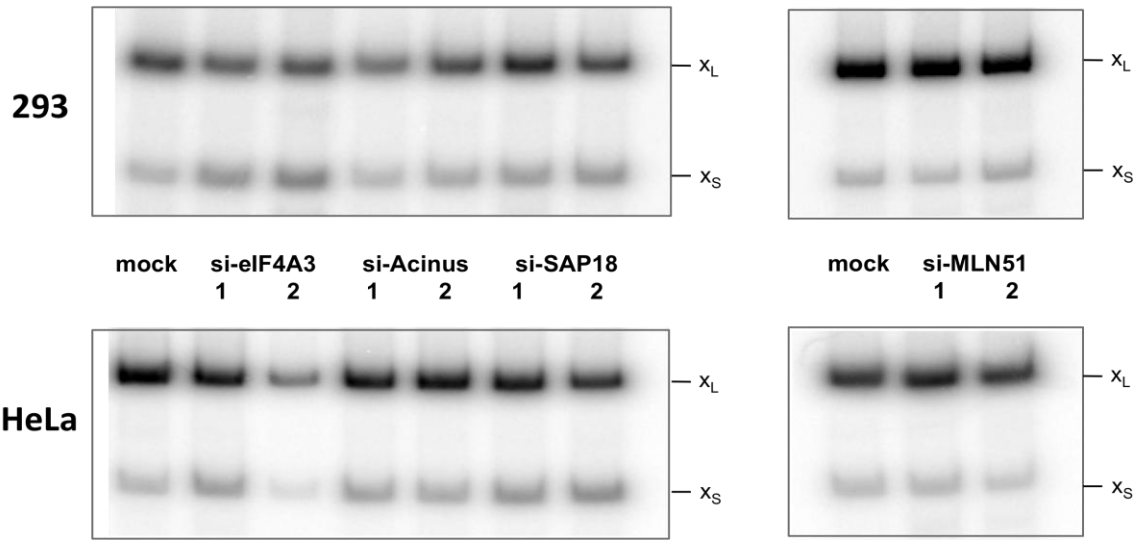

Supplementary figures

S3

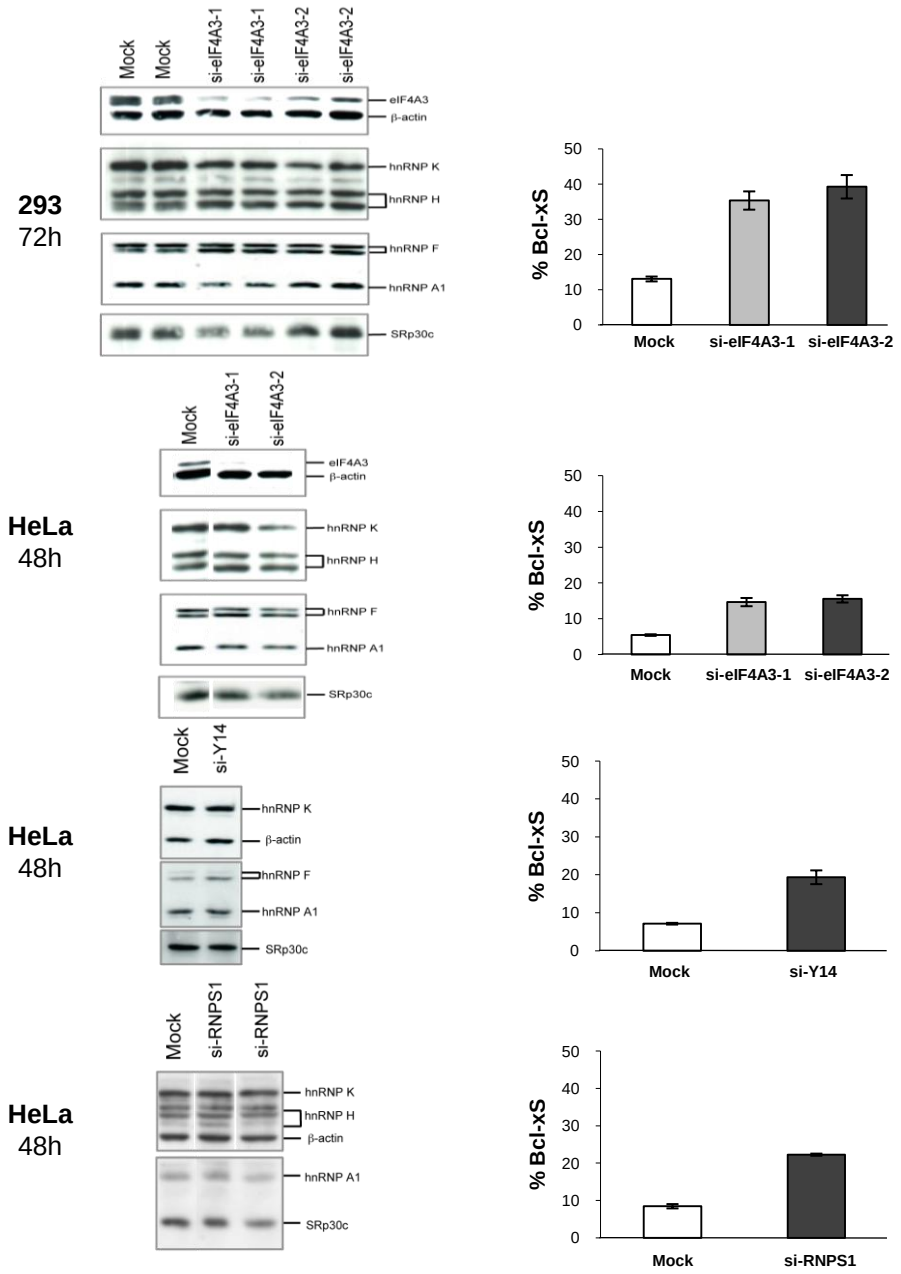

Supplementary figures

S4

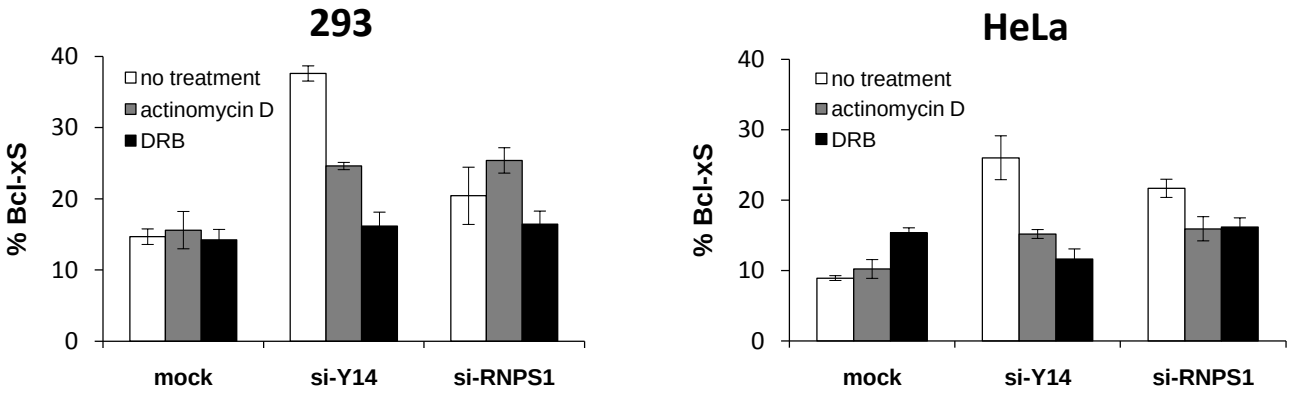

S5

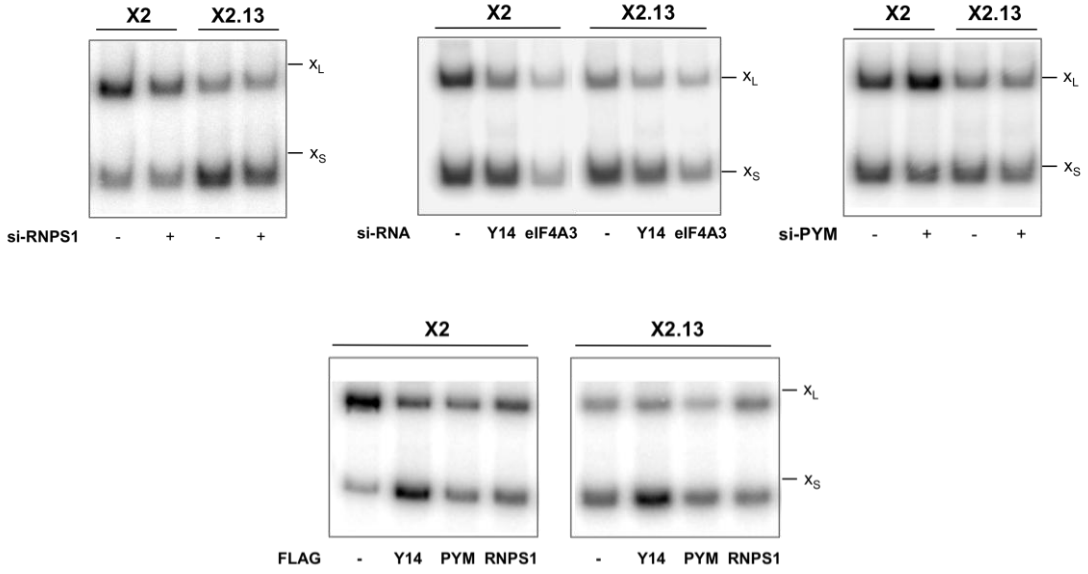

Supplementary figures

S6A

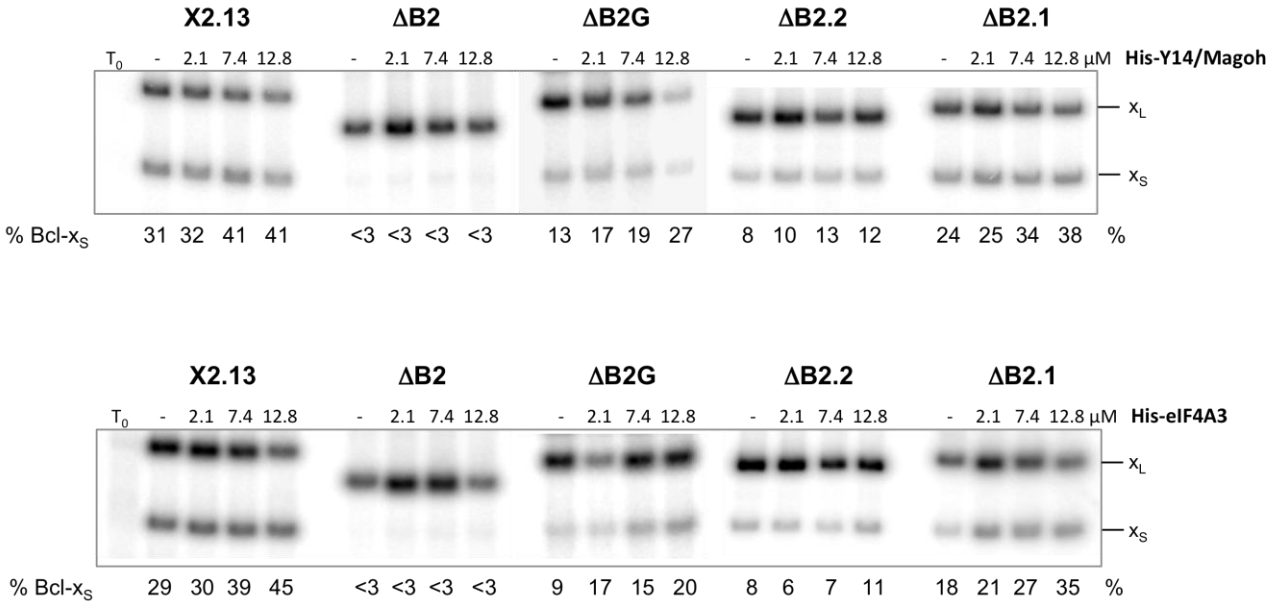

S6B

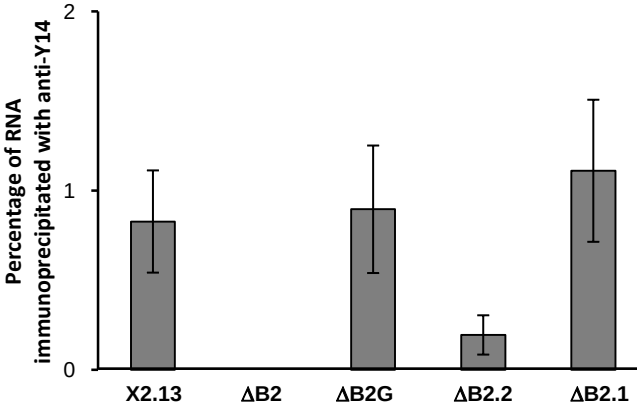

S6C

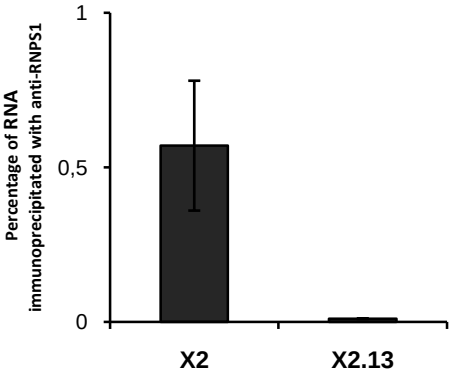

Supplementary figures

S7

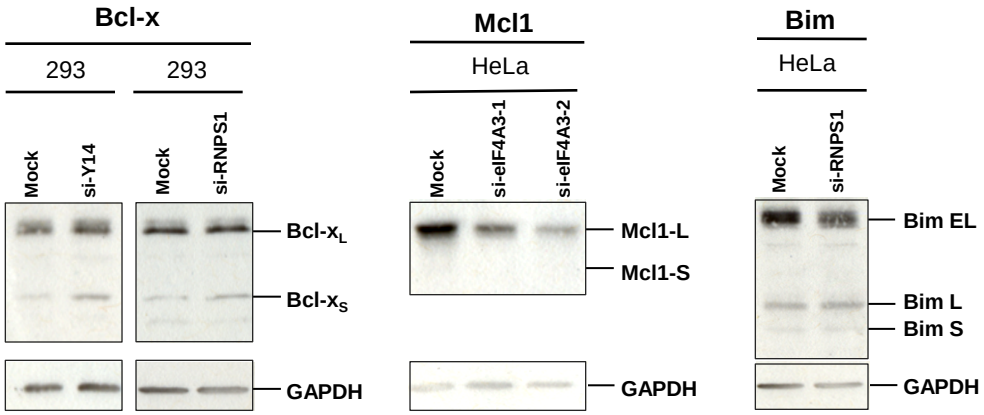

Supplementary figures

S8A

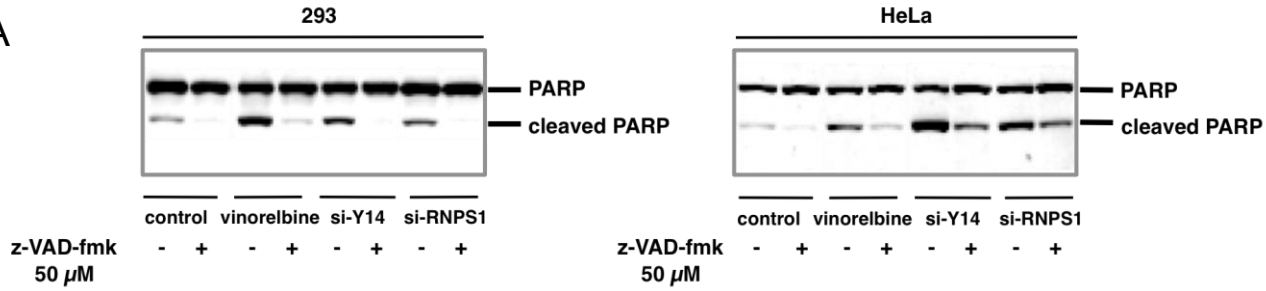

S8B

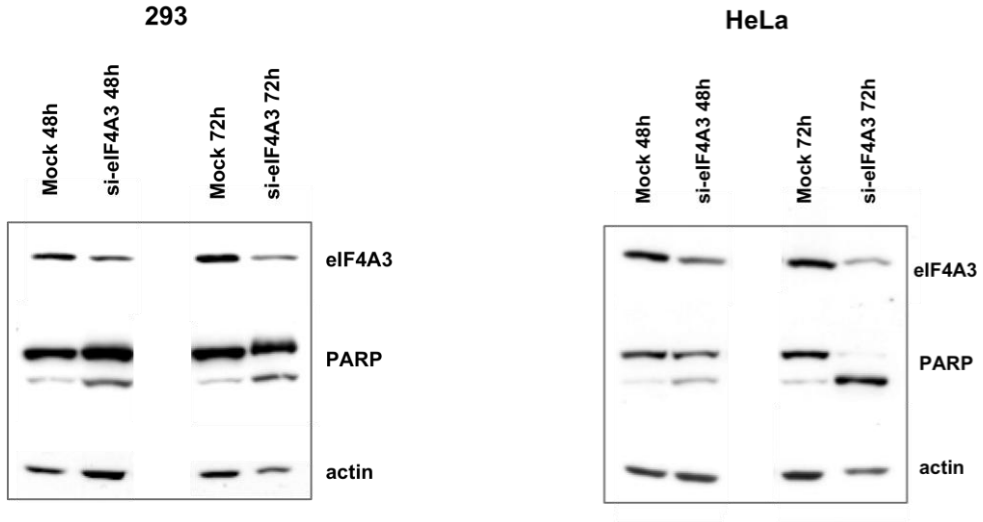

S8C

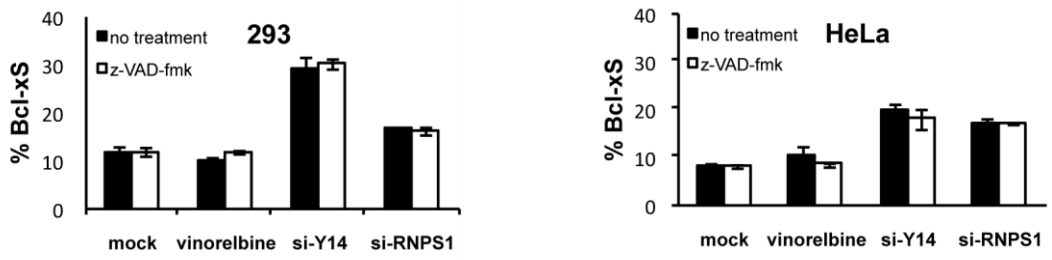

Supplementary figures

S9

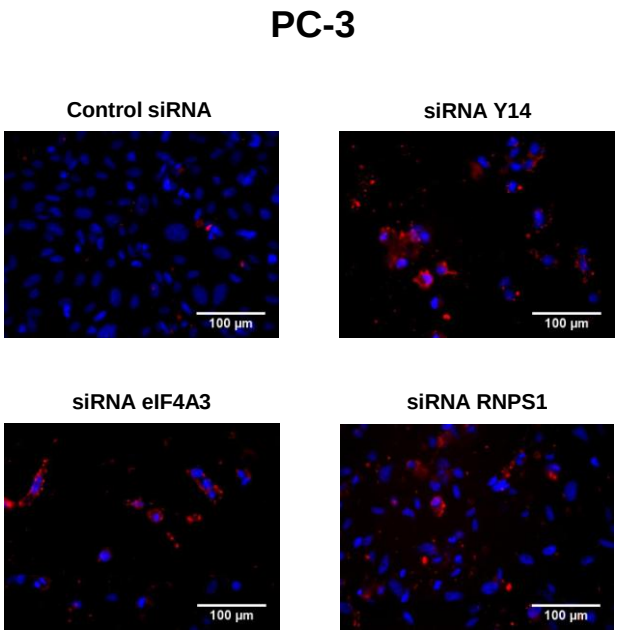

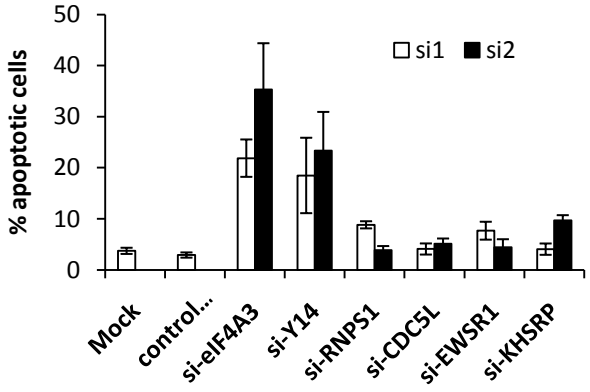

Supplementary Table 1

	PC3	MDA-MB-231
hnRNP F		
hnRNP H		
hnRNP K	x	x
hnRNP A1		
hnRNP A2		
hnRNP L		
U2AF1		
U2AF2		
PRPF4B		
PRPF8		
SF3B4		
SF3A1		
SF3A2		
Y14	x	x
RBM25		
RBM10		
RBM5		
RBM6		
RBM9		
RBMS1		
RBPMS		
RNPS1	x	x
MLN51		
DDX6		
DDX39		
eIF4A2		
FUS		
KHSRP		
Sam68		
SFPQ		
Raly		
SRPK1		
SFRS16		
SFRS14		
SFRS10		
RNPC2		
BRCA1		
HMGA1		
THOC1		
EWSR1		
TAF15		
FXR1		
ZNF638		
CTNNB1		
Nono		
FIP1L		
TIAL1		
RPL22		
CDK11		
MBNL1		
FMR1		
SNRP70		
NOVA		
CDC5L		
CUGBP1		
DEK		
CRK7		
CCNH		
NPM1		
SAFB		
SRA1		

Supplementary Table 2

Gene	Sequence siRNA_1	Sequence siRNA_2
ACINUS	UUCCAUCAGUAUCACCACUTT	GCUCGCUGCCCAAAUCAUUTT
ALY/REF	GGCAGCACGAUCUUUUCGATT	GCACGAUCUUUUCGACAGUTT
BRCA1	CAGCUUGACACAGGUUUGGTT	ACCCGAAAAUCCUUCCUUGTT
CCNH	GGUACGGCUUGUAUGUAUUTT	UACGGCUUGUAUGUAUUUCTT
CDC5L	GCACAUUACCUAUCUGGAATT	GUUUGGUACCAAUAAUUCATT
CDK11	CACCGUGCAUCAAAAGCAATT	CUUACUUUACCAGAUUCUUTT
CRK7	CACCGAAGUGUUGUUAACATT	CCAUUCGUGAAAUCAAAAUTT
CTNNB1	GUUAUCAGAGGACUAAAUATT	GUACCGGAGCCCUUCACAUTT
CUGBP1	CAGAUCUUGAUGCUAUCAATT	CUUGCGGGAACUCUUCGAATT
DDX39	CGAUCUUUUGGAUUACGAUTT	GGCUCCUCAAGAGAGCACATT
DDX6	CUCUACUGACUUUCAAAAGTT	ACGUGAGUGAAUUCAGAUATT
DEK	AAAGGAAGUGUCCAAUAUATT	GAAUGUGGGUCAGUUCAGUTT
EIF4A2	GGCUGAAGCACCACAUAUUTT	GGCACUUGGAGACUAUAUGTT
EIF4A3	AGCCACCUUCAGUAUCUCATT	GCUCUCGGUGACUACAUGATT
EWSR1	CCACUGAUGUCAGCUAUACTT	AAGCUAUGGAACCUAUGGATT
FIP1L	GCGUCACAGAGCAAGUCGATT	GACGACACAGGGAGAAAGATT
FMR1	CACUGCUAUUGAUCUAGAUTT	CCUCGAGAUUUCAUGAACATT
FUS	GGACAGCCCAUGAUUAAUUTT	GGCAACGGUCUCUUUUGAUTT
FXR1	GUACGAAGUUGAUGCUUAUTT	UUGCGAAGUAUUCGUACGATT
HMGA1	CCACAACUCCAGGAAGGAATT	CACAACUCCAGGAAGGAAATT
HNRNPA1	CCACUUAACUGUGAAAAAGAUTT	AACUUUGGUGGUGGUCGUGCATT
HNRNPA2	AAGCUUUGAAACCACAGAAGATT	AAGAAGCUGUUUGUUGGCGGATT
HNRNPF	GCGACCGAGAACGACAUUUTT	GGAAGAAAUUGUUCAGUUCTT
HNRNPH	GCACAGGUAUAUUGAAAUCTT	GGAAGAAAUUGUUCAGUUCTT
HNRNPK	GAGCGCAUAUUGAGUAUCATT	UCUAGCAGGAGGAAUUAUUTT
HNRNPL	GCACUCUGAAGAUCGAAUATT	UAUGGCUUGGAUCAAUCUATT
KHSRP	GCACCGUGCAGGAGAUCAUTT	GCGGGGAGACCAUUAAGCATT
MBNL1	GACGCAAUAACUUGAUUCATT	AAACGCAGUUGGAGAUAAATT
MLN51	CUCGGAUUAUGAAAGUGCATT	CCAGCAUACAUACCUCGGATT
NONO	GACUAUUGACCUGAAGAAUTT	CCUGCAAAUGGGCAACAGGTT
NOVA	AGGUUCUCAUACCUAGUUATT	GCUGCUGGAUCUAUAAUUGTT
NPM1	AAUGAGCACCAGUUAUCUUTT	CACUUUAAGGUGGAUAAUGTT
PRPF4B	CCUAUAGUCAGCAGUUGUUTT	CUUACGAGAGGUGUUAAAATT
PRPF8	GAGAUAGGAGGCAUUUCAATT	CGCCGAGAAAAAAGAGAUATT
RALY	GCAAGCAAUGUAACCAACATT	CUCUCGAGUCUUCAUUGGATT
RBM10	AAGGUGUCGAUGCACUACATT	GCAUUGUAACGCCUAUCGATT
RBM25	AGGAGAGAUCAGAUGAUUATT	CUGUCACUAAUGACGAUGATT
RBM5	GAUACGGUUCCAUCAUAGATT	UAGUACGGCUAUUGCUGCUTT
RBM6	UCGACCUGCUAACAGAACUTT	ACCGAUCUUCCUGUUCAUUTT
RBM9	CACCUCCGCAGAAUGGAAUTT	CAGACACAAAGUAGUGAAATT
RBMS1	CUGAUGGAGGACAGAAAAATT	GAAGACCAUGGCAUAGAGATT
RBPMS	CUACGACUAGAGUUUGCUATT	CCGCUUCGAUCCUGAAAUUTT
RNPC2	GCGGCAAGAAUUCGACCAATT	GAUGCAAGGACAGUCUUCUTT
RNPS1	UCUCGGUCCAGCUCGACUUTT	GCAUCCAGCCGCUCAGGAATT
RPL22	UGGUGAAGGGGGGCAAAAATT	GCAAGUUCUGAAGUUCACUTT
SAFB	CCGAACGGACUGUAGUAAUTT	AGGGGUGCCUGUGAUUAGUTT
SAM68	CGAGUGCUGAUACCUGUCATT	UGAUGGAUGAUAUCUGUCATT
SAP18	CGGGUCUUCACCACCAAUATT	GGCGCAUGAGACCAUAUUATT
SF3A1	CUGACAUCUUCGGUGUAGATT	CUGAGCGGCGUACUGACAUTT
SF3A2	GACCCGUACUUCAUGAAGATT	AUGCAAACUCUGCCUGACATT
SF3B4	GUAGCUCCUUGGGGCAAAGTT	GGCAAAGGUACUAAUCCCUTT
SFPQ	ACAGCCGAAUGGGCUACAUTT	UUCGUCAACGUGAGAUGGATT
SFRS10	UCACGUAGCAGGUCUUACATT	GUCUUACAGUCGAGAUUAUTT
SFRS14	UUCGAUGUGUUCCGACAGATT	GAAAUCACUUAGAGAAUUGTT
SFRS16	GUACCAGAUCUACAUUGAUTT	UGUACCAGAUCUACAUUGATT
SNRP70	CACCACAAUCAACCUUAUUTT	GGUGUACGGACCUAUCAAATT
SRA1	CCACAGUCGAACUCCUCUATT	CCACGUCUGACAAGAGAGATT
SRPK1	AGGUUAUCAUCUUGUGAAATT	ACCAUGUGAUCCGAAAGUUTT
TAF15	GGAUUAUGGACCCAGAACATT	GUGUCUACAGAUCAAGUUGTT
TAP	GGCUCCUGAGCAUGAUUCATT	AGCAGCUUAGCCGAGUAUUTT
THOC1	GUCGACACAUCCUGUUGCATT	GGCAGGUCAAAUUCAAAAGTT
TIAL1	GAUAUGGUAUGGCAAGUUATT	GUAAACCAGUCAAGUCCAATT
U2AF1	GCUCUCGGUUGCACAAUAATT	GAAUAACCGUUGGUUUAAUTT
U2AF2	GCUCAACGAGAAUAAACAATT	AGGUCCUGUGCCUCAUGAATT
UAP56	AAGGGCUUGGCUAUCACAUUU	GUCACACUCGGGAGUUGGCTT
Y14	CCACCGAAGAAGACAUACATT	GGAUGCGUGAGGAUUAUGATT
ZNF638	AGCAUUAGAAGAUGUAGUATT	CGCUACAAAGAGUGAUUCATT